

Development of droop control with active power limitation and dc voltage limitation for multiterminal high-voltage direct current system

Toru Yoshihara | Mamoru Kimura

Research & Development Group, Hitachi Ltd., Hitachi, Japan

Correspondence

Toru Yoshihara, Research & Development Group, Hitachi Ltd. 7-2-1, Omika-cho, Hitachi 319-1221, Japan.
Email: tohru.yoshihara.fe@hitachi.com

Translated from Volume 139 Number 12, pages 731–736, DOI: 10.1541/ieejpes.139.731 of *IEEE Transactions on Power and Energy* (Denki Gakkai Ronbunshi B)

Abstract

As for the offshore wind farm connected multiterminal high-voltage direct current system, this paper proposes the new droop control scheme for onshore converters with active power limitation and dc voltage limitation, and then the simulation results with three-terminal high-voltage direct current system model are shown.

KEY WORDS

droop control, high-voltage direct current, multiterminal

1 | BACKGROUND

Wind farms (WFs) have been increasingly introduced in order to reduce environmental load. High-voltage direct current (HVDC) power transmission and multiterminal HVDC (MTDC) power transmission draw attention as means to transmit power generated by WF to onshore grids.^{1–4} In Japan, too, technical development of WF-connected MTDC (WF-MTDC) systems has advanced¹; particularly, the authors have studied control and protection of multivendor WF-MTDC systems.^{5–10} One of the issues in WF-MTDC operation is power flow control within dc grids. Power generated by a WF is constantly changing with wind conditions, and WF-MTDC systems should provide flexible and autonomous control of power received at the onshore side according to WF output variation, while meeting operational constraints of both onshore and dc systems. There are a number of methods for power flow control within dc grids, such as master-slave control and voltage droop control, to set operating characteristics of active power and dc voltage at the onshore side.¹¹ With these methods, commands of active power and dc voltage as well as droop slope, and other parameters are sent to onshore terminals, and each terminal operates autonomously according to these commands so as to realize power flow control in the whole dc grid.

However, constraints on received power at the onshore side cannot be taken into account using only existing methods such

as master-slave control and voltage droop control. In addition, command values needed to set master-slave control and voltage droop control are different for each method, while from the operator's standpoint, switching among multiple operation schemes should be possible by just modifying command values.

In this context, the present paper proposes a new method of droop control with limitation of active power and dc voltage, and reports on evaluation results obtained through simulations on a three-terminal HVDC system.

2 | POWER DISPATCH CONTROL IN WF-MTDC

2.1 | Configuration example of WF-MTDC

An example of WF-MTDC configuration is shown in Figure 1. This configuration is a three-terminal WF-MTDC in which an offshore WF is connected via terminal WF to two terminals A and B at the onshore side. WF-MTDC is provided with a central control system that performs centralized control of the entire system. In this configuration, the terminals A and B are also connected by dc so that the three terminals form a loop. Modular multilevel converter (MMC) featuring easy voltage upgrade and low harmonic content is assumed as the ac-dc converter in the substation.

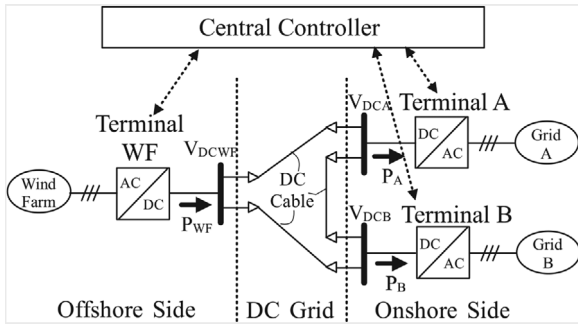


FIGURE 1 Example of WF-MTDC

2.2 | Operating characteristics of active power and dc voltage

WF power output continuously fluctuates with wind conditions. Thus, in WF-MTDC operation, dc voltage at the onshore side must be appropriately controlled according to fluctuations of power fed from offshore WF, and power dispatch control is necessary to appropriately distribute active power received at each terminal depending on the operation conditions of the onshore grid.

In WF-MTDC, power dispatch control in dc grid is realized through an autonomous decentralized control scheme in which constant power control (automatic active power regulator [APR]) following WF output is applied to the offshore terminals, while each onshore terminal is controlled autonomously based on assigned operating characteristics of active power and dc voltage. With regard to operating characteristics of active power and dc voltage, there are following three basic control strategies¹¹:

- master slave method (MSM),
- voltage margin method: (VMM),
- voltage droop method: (VDM).

First, we will discuss MSM. Reference voltage of dc grid is set by applying constant dc voltage operation (dc automatic voltage regulator [DCAVR]) to one of onshore terminals, while the other onshore terminals are operated with APR to control power flow in the dc grid. In this method, power inflow/outflow at DCAVR terminal equals the total of power inflow/outflow at the other terminals. In so doing, only one DCAVR terminal is set, as a rule, in a MTDC system because coexistence of two or more DCAVR terminals would bring about interference.

Next, we will consider VMM. With this strategy, each terminal switches between DCAVR mode and APR mode depending on self-terminal dc voltage. A feature of VMM control is that to switch between DCAVR and APR modes, dc voltage is set differently for each terminal. Due to the different setting of reference voltage at each terminal, even in case of DCAVR terminal drop, another terminal takes over DCAVR

operation to re-establish reference voltage of dc grid. In so doing, reference voltage changes discretely.

Finally, we will discuss about VDM. This is a control strategy to provide a droop to operating characteristics of self-terminal dc voltage and active power. As distinct from the two control methods described above, reference voltage of dc grid is not established by DCAVR terminal; instead, power flow control in dc grid is performed while moderately changing dc voltage in the entire system. In VMM, reference voltage changes stepwise, while in VDM, dc voltage changes continuously according to the droop characteristic of each terminal.

MSM, VMM, and VDM have respective merits and demerits, but in literature,¹² for example, VDM strategy is acknowledged as the most suitable for power flow control in WF-MTDC.

- With MSM, there is a risk of total system shutdown in case of DCAVR terminal drop.
- With VMM, dc voltage to switch between DCAVR and APR modes must be gradually shifted across all onshore terminals. Therefore, operational range of dc voltage increases with more onshore terminals. For example, in case of 10 onshore terminals and reference voltage shift of 0.03 pu, operational range of dc voltage has to be expanded to $0.03 \times (10 - 1) = 0.27$ [pu].

In addition to the three mentioned strategies, there are many other approaches to operating characteristics of active power and dc voltage, such as multistage MSM and dead-band VDM etc.^{13–15}

3 | DROOP CONTROL WITH LIMITATION OF ACTIVE POWER AND DC VOLTAGE

3.1 | Proposed operating characteristics

This study re-examined droop characteristics with limitation of active power and dc voltage as operating characteristics that make it possible to obtain setting parameters from a centralized control system that covers the entire MTDC, and to switch over among control strategies such as MSM, VMM, and VDM. Droop control characteristics with limitation of active power and dc voltage are illustrated in Figure 2.

With the droop characteristics in Figure 2, operating characteristics are defined by the following seven parameters. These parameters are values that can be set online from a centralized control system:

- reference operating point (P_{REF}, V_{DCREF}),
- droop control slope (K_{DR}),
- upper/lower limit of active power (P_{LLIM}, P_{ULIM}),

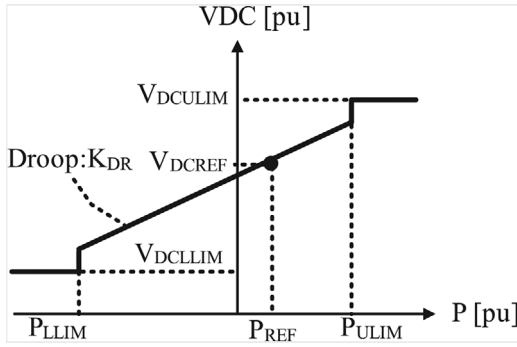


FIGURE 2 Droop control characteristics with active power (P) limitation and DC voltage (V_{DC}) limitation

TABLE 1 Example of setting parameters of proposed droop control

Inputs	Case (a)	Case (b)	Case (c)
P_{REF}	0.0	1.0	0.0
V_{DCREF}	1.0	1.0	1.0
K_{DR}	0.0	∞	2.0
P_{ULIM}	∞	∞	0.1
P_{LLIM}	$-\infty$	0.0	-0.1
V_{DCULIM}	1.0	1.1	1.12
V_{DCLLIM}	1.0	0.9	0.88

- upper/lower limit of dc voltage (V_{DCLLIM} , V_{DCULIM}).

In addition, capacity constraint on received power in the onshore grid side, operating range of dc voltage, and other settings can be realized via constraint on upper/lower limit of received power on the onshore grid side, upper/lower limit of dc voltage, etc. Moreover, MSM, VMM, and VDM can be modified online through parameter settings. An example of parameter settings is given in Table 1, and corresponding operating characteristics are illustrated in Figure 3. Here all parameters are in per unit. For example, DCAVR characteristics can be imitated by setting equal values for V_{DCREF} , V_{DCULIM} , V_{DCLLIM} as in Case (a), while APR mode can be imitated by setting equal values for P_{REF} , P_{ULIM} , P_{LLIM} as in Case (b). In contrast, when voltage limits V_{DCULIM} and V_{DCLLIM} are set differently at each terminal, even if some terminal drops, another terminal takes over voltage determination to re-establish reference voltage in dc grid, as with VMM. Besides, the range of received power at the onshore side can be restricted by setting P_{ULIM} and P_{LLIM} in droop characteristics.

3.2 | Droop control with limitation of active power and dc voltage

In order to reflect droop characteristics with limitations of active power and dc voltage in converter control, droop

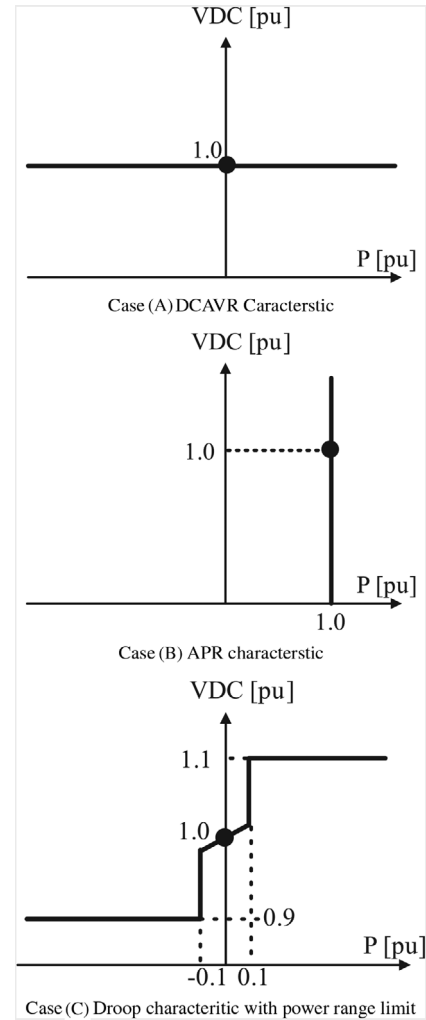


FIGURE 3 Example of operation characteristics of proposed droop control

control with limitations of active power and dc voltage is added to MMC converter control at the onshore side.

First, let us explain MMC converter control. In this paper, MMC converter control, including current control system, capacitor voltage control, and other elements, is configured based on literature.^{16–18} For this reason, detailed explanations are omitted, and description of MMC converter control is kept to a minimum. In MMC converter control, active power command P^* , reactive power command Q^* , and other operation commands are obtained, and AC voltage command V_{AC}^* and dc voltage command V_{DC}^* are calculated so that converter outputs P^* and Q^* . Then, based on V_{AC}^* and V_{DC}^* , activation pulses for MMC unit cells are calculated in PWM control and sent to the unit cells.

Next, let us explain droop control with limitations of active power and dc voltage with reference to Figure 4. First, offset ΔV_{DC}^* of dc voltage command is determined based on active power P_{det} detected on converter's dc side (P_A , P_B in Figure 1) and setting parameters of droop control with active power/dc

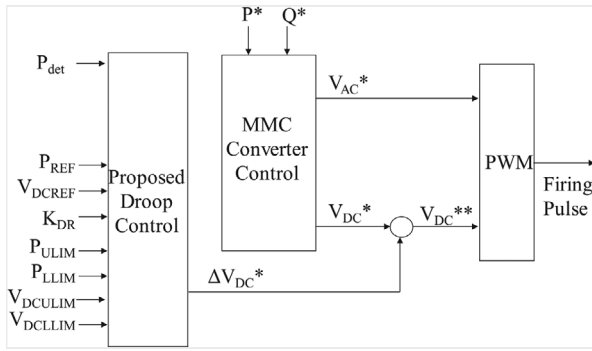


FIGURE 4 MMC control block with proposed droop control

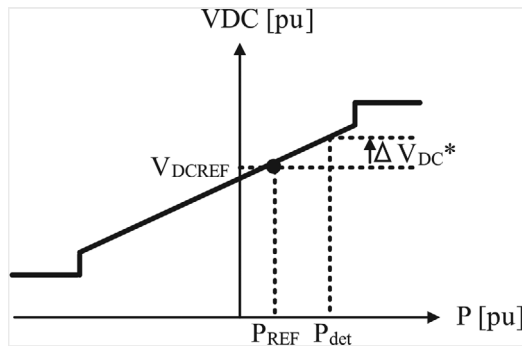


FIGURE 5 ΔV_{DC}^* calculation

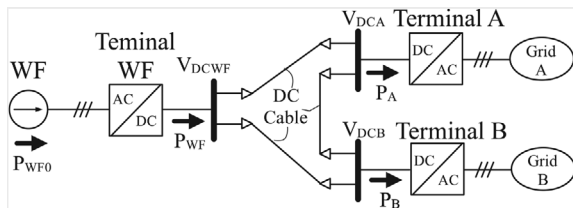


FIGURE 6 Model grid

voltage limitations. As shown in Figure 5, ΔV_{DC}^* is obtained with respect to operating point (P_{REF} , V_{DCREF}) and operating characteristics, specifically, as the deviation from V_{DCREF} when active power P_{det} flows. Next, ΔV_{DC}^* is added to dc voltage command V_{DC}^* of MMC control to obtain V_{DC}^{**} . Based on the dc voltage commands V_{AC}^* and V_{DC}^{**} , activation pulses for MMC unit cells are calculated in PWM control and sent to the unit cells. Thus, droop control with limitations of active power and dc voltage is realized.

4 | SIMULATIONS

4.1 | Model system

The model grid is shown in Figure 6, and its parameters are listed in Table 2. Maximum output of offshore WF is 500 MW. All converters are assumed as MMCs rated at power output

TABLE 2 Model grid parameters

Parameters	Value	Unit
WF maximum power	500	MW
Converter rated capacity	528	MVA
Converter rated power	500	MW
Rated DC voltage	500	kV
DC line length	100	km
DC line resistance	0.01	Ω/km
DC line inductance	0.29	mH/km
DC line capacitance	0.20	$\mu\text{F}/\text{km}$

TABLE 3 Setting parameters of P - V_{DC} control characteristics in this simulation

Inputs	Terminal A	Terminal B	Unit
P_{REF}	0.4 \Rightarrow 0.7	0.2 \Rightarrow 0.3	[pu]
V_{DCREF}	1.0	1.0	[%VDCpu/%Ppu]
K_{DR}	2.0	20.0	[pu]
P_{ULIM}	0.6 \Rightarrow 0.8	0.201 \Rightarrow 0.4	[pu]
P_{LLIM}	0.0	0.0	[pu]
V_{DCULIM}	1.12	1.1	[pu]
V_{DCLIM}	0.88	0.9	[pu]

of 500 MW and dc voltage of 500 kV; WF is imitated by a current source. Each of the three dc cables is 100 km long. The following explanations are in per unit, 500 MW and 500 kV defined as 1.0 pu.

4.2 | Simulation conditions

Simulations were conducted in this study with WF output surge and varied parameters of active power/dc voltage in order to evaluate operation of substations with respect to operating characteristics set in droop control. Specifically, P_{WF0} was abruptly increased from 0.6 to 1.0 pu at the moment $t = 0.5$ s, and active power/dc voltage parameters were changed at the moment $t = 2.0$ s. Parameters of active power and dc voltage at terminals A and B are given in Table 3. In the table, parameter changes at $t = 2.0$ s are shown by the arrows.

The changes in power received at terminals A and B and in dc voltage as assumed in the simulations are explained in Figure 7. The diagrams illustrate active power and dc voltage characteristics at terminals A and B in each time slice, namely, (a) initial state, (b) after WF output surge, (c) after change in active power and dc voltage. Operating points of terminals A and B in each time slice are shown by triangles and circles, respectively. With converter loss, dc line transmission loss, and voltage drop ignored at each terminal, respective operating points can be derived from the relations $V_{DCA} = V_{DCB} = V_{DC}$, and $P_{WF0} = P_A + P_B$.

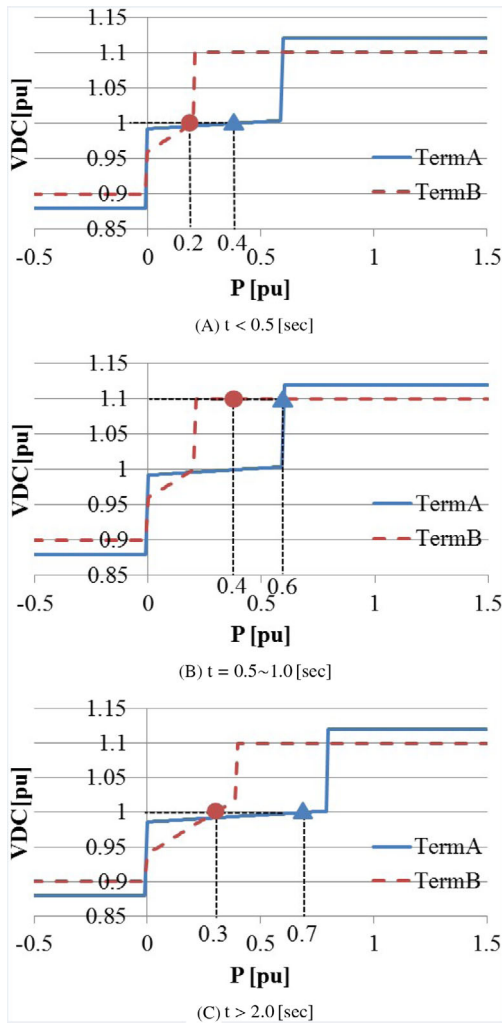


FIGURE 7 P - V_{DC} control characteristics in each period [Color figure can be viewed at wileyonlinelibrary.com]

Based on the operating characteristics of Figure 7, steady-state active power and dc voltage assumed in the simulations are shown along the time axis in Figure 8. Instantaneous value analysis was performed to check how the assumed results of Figure 8 compare with the simulated results.

4.3 | Simulation results and discussion

The simulation results are presented in Figure 9. The graphs show, top to bottom, active power received from dc grid at each terminal and dc bus voltage; the symbols correspond to those in Figure 6. First, when the surge of WF output at $t = 0.5$ s, it results in changes of active power and dc voltage at each terminal. At the moment $t = 2.0$ s, PA is 0.62 pu and PB is 0.37 pu; as compared to the assumed results of Figure 8, the error is greater for PB (0.03 pu). The errors can be explained by the fact that the results of Figure 8 are calculated using a model ignoring losses in converters and dc cables as well as voltage drop. The same pertains

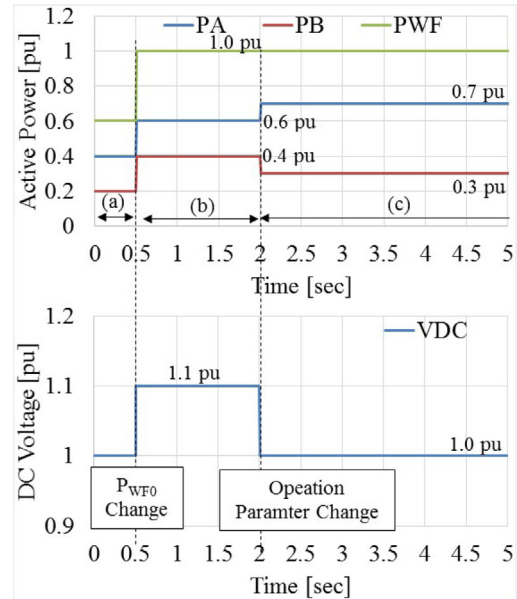


FIGURE 8 Assumed changes of P and V_{DC} [Color figure can be viewed at wileyonlinelibrary.com]

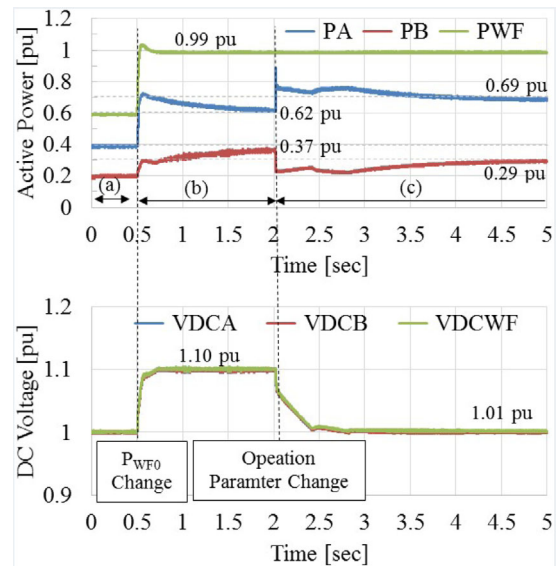


FIGURE 9 Simulation results of P and V_{DC} [Color figure can be viewed at wileyonlinelibrary.com]

to convergence at 5.0 s after operating characteristics were changed at 2.0 s. In addition, the assumed results in Figure 8 do not involve control response, control interference between the terminals, etc. On the other hand, these factors are involved in the instantaneous-value analysis; thus, follow-up delays of 1-2 s after the changes of WF output and operating parameters can be seen in Figure 9, but the values eventually converge to those assumed in Figure 8.

The simulations with WF output surge and changes in active voltage/dc power confirmed that substations operate

according to the operating characteristics set in droop control with limitations of active power and dc voltage.

5 | CONCLUSION

In WF-MTDC power flow control, it is desirable to provide autonomous decentralized control at onshore terminals according to WF output fluctuations, and to adjust onshore operating characteristics to commands from a centralized control system. In this context, the present paper proposed droop control with limitation of active power and dc voltage; the proposed control supports constraints on power received by onshore grid, and makes it possible to switch over among operation modes (MSM, VMM, and VDM) simply by changing command values. In addition, an instantaneous value analysis model of a three-terminal HVDC system was built to verify whether substations operate according to operating characteristics set in the droop control with limitation of active power and dc voltage. Simulations with WF output surge and changes of active power/dc voltage characteristics confirmed that all substations operate according to the set characteristics.

Effectivity of the proposed droop control was confirmed via simulations with the parameters listed in Table 3. However, in real operation, the parameters of Table 3 must be set with regard to abrupt changes of WF output as well as faults in ac and dc grids. In addition, depending on the operating conditions, operating points are not necessarily determinable by only means of droop characteristic settings, and combination with WF output curtailment may be required. We will further explore methods to calculate settings of droop characteristics for arbitrary operating conditions as well as combining droop control with WF output curtailment.

Results of this study were obtained in the framework of a project commissioned by the New Energy and Industrial Technology Development Organization (NEDO).

REFERENCES

1. Ugalde-Loo CE, Adeuyi D, et al. Lessons learnt from the BEST PATHS project for the integration of offshore wind power plants using multi-terminal HVDC grids. *CIGRE 2018*, B4-113, August 26-31, Paris, France, 2018.
2. Irnawan R, Silva FMFD, Bak CL, Lindefelt AM, Alefragkis A. DC grid control concept for expandable multi-terminal HVDC transmission systems. *CIGRE 2018*, B4-115, 26 August 26-31, Paris, France, 2018.
3. Tang G, Wang G, He Z, et al. Characteristics of system and parameter design of key equipment for Zhangbei DC grid. *CIGRE 2018*, B4-121, August 26-31, Paris, France, 2018.
4. Despouys O, Rault P, Burgos A, Vozikis D, Guillaud X, Larsson T. Assessment of interoperability in multi-vendor VSC-HVDC systems: interim results of the BEST PATHS DEMO #2. *CIGRE 2018*, August 26-31, B4-134, Paris, France, 2018.

5. NEDO. On implementation structure of “next Generation offshore HVDC system” (2015.6.30). http://www.nedo.go.jp/koubo/FF3_100136.html. (In Japanese)
6. Suwa H, Arai T, Ishiguro T, et al. PSCAD/EMTDC and RTDS simulation analysis of multi-vendor multi-terminal HVDC system connected to offshore wind farms. *IPEC 2018 ECCE ASIA*, 22F3-2, May 20-24, Niigata, Japan, 2018.
7. Yoshihara T, Kimura M. A basic study on operation of offshore HVDC system at a system fault. *2017 National Conference of IEE Japan*, 6–202, 2017. (In Japanese)
8. Yoshihara T, Kimura M. A basic study on braking chopper control in offshore HVDC system. *2017 Conference of IEE Japan PE Society*, 150, 2017. (In Japanese)
9. Yoshihara T, Kimura M. A basic study on braking chopper control in multi-terminal HVDC system. *2017 Natational Conference of IEE Japan*, 6-202, 2017. (In Japanese)
10. Yoshihara T, Kimura M. A basic study on droop control with active power/DC voltage limitations in multi-terminal HVDC system. *IEE Japan, PE-18-085, PSE-18-061*, 2018. (In Japanese)
11. Herterm DV, Gomis-Bellmunt O, Liang J. Control principles of HVDC grids. In: Beerten J, Egea A, Vrana TK, eds. *HVDC Grids for Offshore and Supergrid of the Future*. Hoboken, NJ: Wiley IEEE Press; 2016:315-320.
12. TWENTIES. DEMO 3 Requirement specifications. Deliverable n0: 11.1. <http://www.twenties-project.eu/system/files/D11.1%20-%20final.pdf>. Accessed July 18, 2009.
13. Vrana TK, Zeni L, Fosso OB. Dynamic active power control with improved undead-band droop for HVDC grids. *10th IET International Conference on AC and DC Power Transmission (ACDC 2012)*, December 4-5, Birmingham, UK, 2012.
14. Shi X, Li Y, Tolbert LM, Wang F. Cascaded droop control for dc overvoltage suppression in a multi-terminal HVDC system under onshore side AC faults. *IEEE Trans Power Syst.* 2017;32(2):1520-1527.
15. Li H, Liu C, Li G, Iravani R. An enhanced DC voltage droop-control for the VSC-HVDC grid. *10th IET International Conference on AC and DC Power Transmission (ACDC 2012)*, 4-5 December, Birmingham, UK, 2012.
16. Hagiwara M, Maeda R, Akagi H. Theoretical analysis and control of the modular multilevel cascade converter based on double-star chopper-cells (MMCC-DSCC). *IEEEJ Trans IA.* 2011;131(1):84-92. (In Japanese)
17. Fujita H, Hagiwara M, Akagi H. Power flow analysis and DC-Capacitor voltage regulation for the MMCC-DSCC. *IEEEJ Trans IA.* 2016;136(10):768-777. (In Japanese)
18. Inoue S, et al. Laboratory tests of a zero-sequence cancelling modular multilevel cascade converter. *IEEEJ, PE-11*, 2011. (In Japanese)

AUTHOR BIOGRAPHIES



Toru Yoshihara, member, completed his master's course at the University of Tokyo in 2011 (Graduate School of Frontier Science, Department of Advanced Energy) and was employed by Hitachi, Ltd. for the development of large-capacity power electronic devices for power systems.



Mamoru Kimura, member, completed his first term of doctorate at Tohoku University in 1999 (Graduate School of Engineering, Department of Electrical and Communication Engineering), and in 2014 earned the degree of Doctor of Engineer (Tohoku University). In 1999, he was employed by Hitachi, Ltd. And is now in R&D in wind power systems at the Research & Development Group. He is also Dr. Eng. Vice Chairman of Rotating Machinery Technical Committee, IEE Japan and IEEE member.

How to cite this article: Yoshihara T, Kimura M. Development of droop control with active power limitation and dc voltage limitation for multiterminal high-voltage direct current system. *Electr Eng Jpn.* 2020;211:26–32. <https://doi.org/10.1002/eej.23268>